GEOCHRONOLOGY

Open Access

EGU

# Stepwise chemical abrasion–isotope dilution–thermal ionization mass spectrometry with trace element analysis of microfractured Hadean zircon

**C. Brenhin Keller[1], Patrick Boehnke[2], Blair Schoene[3], and T. Mark Harrison[4]**

[1]Department of Earth Sciences, Dartmouth College, Hanover, NH 03755, USA
[2]Eta Vision, Chicago, IL 60611, USA
[3]Department of Geosciences, Guyot Hall, Princeton University, Princeton, NJ 08544, USA
[4]Department of Earth, Planetary, and Space Sciences, University of California, Los Angeles, CA 90095, USA

**Correspondence:** C. Brenhin Keller (cbkeller@dartmouth.edu)

**Abstract.** The Hadean Jack Hills zircons represent the oldest known terrestrial material, providing a unique and truly direct record of Hadean Earth history. This zircon population has been extensively studied via high-spatial-resolution high-throughput in situ isotopic and elemental analysis techniques, such as secondary ionization mass spectrometry (SIMS), but not by comparatively destructive, high-temporal-precision ( $< 0.05\%$ two-sigma) thermal ionization mass spectrometry (TIMS). In order to better understand the lead loss and alteration history of terrestrial Hadean zircons, we conduct stepwise chemical abrasion–isotope dilution–thermal ionization mass spectrometry with trace element analysis (CA-ID-TIMS-TEA) on manually microfractured Hadean Jack Hills zircon fragments previously dated by SIMS. We conducted three successive HF leaching steps on each individual zircon fragment, followed by column chromatography to isolate U–Pb and trace element fractions. Following isotopic and elemental analysis, the result is an independent age and trace element composition for each leachate of each zircon fragment. We observe $\sim 50$ Myr of age heterogeneity in concordant residues from a single zircon grain, along with a protracted history of post-Hadean Pb loss with at least two modes circa $\sim 0$ and 2–4 Ga. Meanwhile, stepwise leachate trace element chemistry reveals enrichments of light rare earth elements, uranium, thorium, and radiogenic lead in early leached domains relative to the zircon residue. In addition to confirming the efficacy of the LREE-I alteration index and providing new insight into the mechanism of chemical abrasion, the interpretation and rec-

onciliation of these results suggest that Pb loss is largely driven by low-temperature aqueous recrystallization and that regional thermal events may act to halt – not initiate – Pb loss from metamict domains in the Hadean Jack Hills zircons.

## 1 Introduction

Terrestrial zircons with U–Pb ages in excess of 4 Ga were first fortuitously discovered in the Paleoarchean Mt. Narryer quartzite by Froude et al. (1983) and subsequently in greater abundance by Compston and Pidgeon (1986) in a quartz pebble metaconglomerate at the Jack Hills – both in the Narryer Gneiss Complex of the Yilgarn Craton, western Australia. Zircons with Hadean ($> 4$ Ga) $^{207}$Pb/$^{206}$Pb ages have subsequently been reported from most other continents including North America (Bowring and Williams, 1999; Mojzsis and Harrison, 2002; Iizuka et al., 2006), South America (Nadeau et al., 2013; Paquette et al., 2015), Eurasia (Wang et al., 2007; Duo et al., 2007; Xu et al., 2012; Xing et al., 2014), India (Miller et al., 2018), and Africa (Byerly et al., 2018), suggesting a widely distributed occurrence of zircon-bearing crust by at least the late Hadean. Nonetheless, both the antiquity (Valley et al., 2014) and quantity (Holden et al., 2009) of Hadean zircon from the Jack Hills far exceed that yet analyzed from any other locality; as such, the Jack Hills zircon record predominates our understanding of the Hadean eon on Earth.

While the interpretation of petrologic and geochemical data derived from Hadean zircons can be difficult, many constraints have been interpreted to suggest a relatively temperate Hadean eon, featuring liquid water and continental crust (Cavosie et al., 2007; Harrison, 2009; Harrison et al., 2017). Hadean Jack Hills zircons display oxygen isotope compositions enriched in $^{18}O$ relative to the mantle, suggesting a parental magma that incorporated silicates, which have interacted with liquid water (Mojzsis et al., 2001; Wilde et al., 2001; Cavosie et al., 2005; Trail et al., 2007). Unlike lunar and meteoritic zircon (Hoskin and Schaltegger, 2003), Jack Hills Hadean zircons display positive Ce anomalies (Trail et al., 2011; Bell et al., 2016), suggesting conditions sufficiently oxidized to produce $Ce^{4+}$, perhaps associated with magmatic water. Although magma Ti activity is not perfectly constrained for detrital zircons (except in a handful of zircons containing apparently primary rutile inclusions), observed Ti-in-zircon temperatures of $\sim 680\,°C$ are most consistent with a parental magma produced by the water-saturated eutectic melting of pelitic sediment (Watson, 2005; Harrison, 2009). The same Hadean zircons display felsic inclusion suites, including some phases such as apatite, biotite, hornblende, and alkali feldspar (Maas et al., 1992; Hopkins et al., 2010; Bell et al., 2015), that are not abundant or not reported in the host quartzite (Myers, 1988) but are ubiquitous components of granitic magmas. Compounding the above constraints, higher mantle potential temperatures in the Hadean imply lower zirconium abundances for a given magma $SiO_2$, increasing the difficulty of saturating zircon and increasing the volume of felsic crust required to crystallize a given volume of zircon (Keller et al., 2017). If correct, such a relatively uniformitarian Hadean would appear plausibly consistent with independent evidence of subduction-driven flux melting since at least 3.85 Ga (Keller and Schoene, 2018). Nonetheless, a large proportion of the Archean geological community would strongly dispute such views (Condie, 2018; Bédard, 2018), and controversy regarding the nature and origin of Earth's earliest crust is likely to persist. Consequently, much remains to be learned from the terrestrial Hadean zircon record.

To date, the study of the Jack Hills zircons has proceeded in tandem with the development of high-throughput, minimally destructive in situ analytical techniques such as secondary ion mass spectrometry (SIMS) (Froude et al., 1983; Compston and Pidgeon, 1986; Holden et al., 2009). While the high spatial precision and high throughput of these techniques have been critical to the study of the Jack Hills zircons, technical (matrix effects, mass and elemental fractionation) and mathematical (counting statistics) constraints frequently impose an effective trade-off between spatial and temporal precision.

Consequently, while Hadean $^{207}Pb/^{206}Pb$ ages are frequently resolved to the $\pm 0.5\%$ level, there is a limit to the extent to which the concordance of the independent $^{206}Pb/^{238}U$ and $^{207}Pb/^{235}U$ chronometers (and thus our con-

fidence that a measured age reflects closed-system behavior) can be established with in situ methods. Such limitations are particularly relevant when attempting to identify early open-system behavior (i.e., Pb loss or Pb gain that occurs closer to the crystallization age than to the present day), which will move samples nearly parallel to concordia (Wetherill, 1956). Early Pb remobilization during Archean ultrahigh-temperature (UHT) metamorphism has been observed in at least one case to produce spurious apparent Hadean $^{207}Pb/^{206}Pb$ ages in Eoarchean zircons from UHT granulites of the Napier Complex, Enderby Land, Antarctica (Kusiak et al., 2013; Kelly and Harley, 2005). However, such extreme effects have been ruled out in the Jack Hills zircons (Valley et al., 2014), which do not appear to have undergone greater than greenschist facies metamorphism (Trail et al., 2016). Even so, early Pb mobility – particularly Pb loss – has often been considered a limitation when interpreting Hadean zircon hafnium isotope systematics (Guitreau and Blichert-Toft, 2014; Bell et al., 2014; Whitehouse et al., 2017)

While once requiring large multigrain zircon aliquots, the average mass of sample used in a bulk isotope dilution TIMS U–Pb analysis decreased by more than 5 orders of magnitude between 1975 and 2010. Over the same period, temporal precision improved by over an order of magnitude, all due to improvements in analytical techniques and instrumentation (Schoene, 2014). In total, we may now expect to obtain $< 0.05\%$ relative temporal precision and accuracy on a single $< 1\,\mu g$ fragment of Hadean zircon ($\sim 300\,pg\,U$), providing a precise and accurate test of closed-system behavior through concordance.

To improve the likelihood of analyzing closed-system material, zircon fragments intended for ID-TIMS may be first treated with chemical abrasion, which has been observed to selectively dissolve damaged domains likely to have undergone Pb loss (Mattinson, 2005, 2011; Mundil et al., 2004; Widmann et al., 2019). While 12 h of chemical abrasion in concentrated HF at $210\,°C$ is frequently presumed to effectively mitigate Pb loss in zircon, the underlying mechanism and the kinetics of this process remain poorly understood. Moreover, since previously published TIMS ages for Jack Hills Hadean zircons (Amelin, 1998; Amelin et al., 1999) predate the advent of chemical abrasion, it was unknown whether such Hadean zircons could survive the full standard 12 h at $210\,°C$ chemical abrasion procedure. Conducting chemical abrasion in a stepwise manner, whereby intermediate leachates are extracted and retained for analysis, eliminates this risk. By combining such stepwise chemical abrasion with TIMS-TEA, we may obtain matched trace element and geochronological data for each subsequent chemical abrasion step of each analyzed zircon fragment. While time-consuming, such an analytical procedure (Fig. 1) has the potential to provide insight into both the geologic history of Jack Hills Hadean zircon and the efficacy of chemical abrasion.
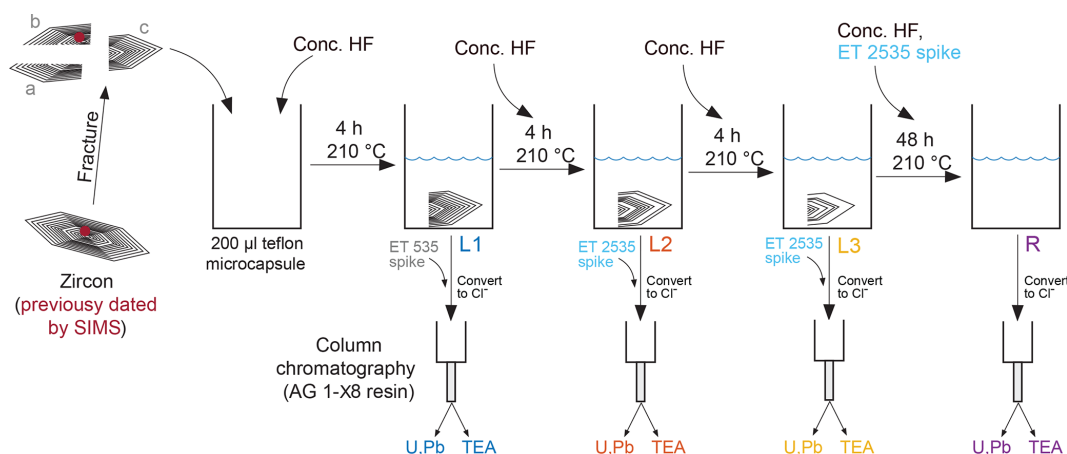
**Figure 1.** Schematic illustration of the step leaching methodology employed in this study. U and Pb fractions separated by column chromatography for each leachate of each zircon fragment were analyzed on an IsotopX Phoenix 62 thermal ionization mass spectrometer, while TEA solutions were analyzed for trace element concentration on a Thermo Element 2 ICPMS at Princeton University.

## 2 Methods

Here we apply stepwise CA-ID-TIMS-TEA (chemical abrasion–isotope dilution–thermal ionization mass spectrometry with trace element analysis) to sub-grain fragments of Jack Hills zircons. Since only some 3 % of Jack Hills zircons have ages > 4.0 Ga (Harrison, 2009), Jack Hills zircons with late Hadean ($\sim$ 4.0–4.1 Ga) SIMS ages were selected from epoxy mounts previously characterized by in situ techniques at UCLA (Table S1 in the Supplement). A total of 23 epoxy-mounted half-zircons were selected for TIMS analysis at Princeton University, 14 of which were further dissected into two to five fragments each by microfracturing with a tungsten carbide point, resulting in a grand total of 54 sub-grain zircon fragments.

To prepare for chemical abrasion (Mattinson, 2005), each zircon fragment was individually loaded into a separate quartz crucible and annealed for 48 h at 900 °C. Annealed zircons were transferred to 3 mL Savillex perfluroacetate (PFA) beakers and moved to a class-1000 clean room where they were rinsed with Milli-Q ultrapure water, transferred to 200 µL Savillex PFA microcapsules, and rinsed with ultrapure HCl. Subsequent analytical steps were conducted in the clean room using class-10 clean hoods, ultrapure reagents distilled in a Savillex DST-1000 sub-boiling still (blank-checked to ensure common Pb concentrations less than 0.1 pg g$^{-1}$), and PFA labware cleaned by heating with alternating ultrapure acids for periods of months to years.

In the first analytical campaign, 36 zircon fragments in separate microcapsules were loaded into two Teflon-lined Parr pressure dissolution vessels with ultrapure hydrofluoric acid (100 µL 29 M HF plus 15 µL 3 M HNO$_3$ per microcapsule, with 5 mL moat HF) and chemically abraded in two steps of 6 h at 210 °C. In the second analytical campaign, the remaining 18 zircon fragments were chemically

abraded in a single Parr vessel in three steps of 4 h, as illustrated in Fig. 1. Between each leaching step, all supernatant acid was extracted, spiked, and retained for analysis (comprising the L1, L2, and L3 leachates). Subsequently, the surviving zircon residue was thoroughly rinsed with H$_2$O, HCl, HNO$_3$, and HF, before finally dissolving any surviving zircon over 48 h at 210 °C with ultrapure HF (as during abrasion) and a measured quantity of isotope dilution tracer. The EARTHTIME $^{205}$Pb–$^{233}$U–$^{235}$U ET535 tracer (Condon et al., 2015; McLean et al., 2015) was used for all L1 analyses, while the EARTHTIME $^{202}$Pb–$^{205}$Pb–$^{233}$U–$^{235}$U double-spike ET2535 was used for the more critical L2, L3, and residue analyses.

After chemical abrasion and dissolution, each of the resulting 54 dissolved zircon residues and 126 leachates was evaporated to dryness, converted to chlorides by heating with ultrapure 6 M HCl, evaporated a second time, and redissolved in ultrapure 3 M HCl to prepare for ion chromatography. For each sample, a small PTFE column was loaded with 50 µL of chloride form Eichrom AG1-X8 anion exchange resin (200–400 mesh), cleaned alternately with H$_2$O and 6 M HCl, and conditioned with 3 M HCl. Following the separation procedure of Krogh (1973) with the modifications of Schoene et al. (2010), samples were loaded and trace elements eluted in 3 M HCl, followed by Pb elution in 6 M HCl and U elution in H$_2$O. Eluted U–Pb separates were evaporated to dryness with $\sim$ 2 µL 0.03 M H$_3$PO$_4$ and stored for analysis.

Isotopic and trace element analyses of the resulting separates were conducted in 2015–2016 at Princeton University. Evaporated U–Pb separates were loaded (U and Pb together) onto zone-refined rhenium filaments with $\sim$ 2 µL silica gel emitter (Gerstenberger and Haase, 1997) for analysis by IsotopX Phoenix 62 TIMS. Thermal ionization mass spectrometry and data reduction procedures were equivalent to those of Schoene et al. (2015), with Pb collected by peak-hopping

on a Daly detector, correcting for a detector dead time of 43.5 ns as determined by repeated analyses of NBS 982 reference material. Where beam intensity allowed, U was collected by static multicollection on Faraday cups with $10^{12} \Omega$ amplifiers; otherwise, U was collected by peak-hopping on a Daly detector, correcting for 37.5 ns dead time as established by repeated analyses of CRM U500. During TIMS analysis, two fragments were identified as contamination introduced during single-fragment annealing and rejected. Isotopic data were processed and analytical uncertainty propagated using Tripoli and U–Pb Redux (McLean et al., 2011; Bowring and McLean, 2011) using a $^{238}U/^{235}U$ ratio of $137.818 \pm 0.045$ (two-sigma) (Hiess et al., 2012). Trace element separates were subsequently analyzed on a Thermo Scientific Element 2 inductively coupled spectrometer (ICPMS) following the procedure of Schoene et al. (2010), with zircon trace element abundances normalized to 496 000 ppm Zr in zircon. Finally, zircon U and Th concentrations were calculated using the zircon Th/U ratio determined from Pb isotopic composition, the ICPMS-derived Th concentrations, and ID-TIMS U and Pb masses. The resulting elemental and isotopic data are tabulated in Tables S1 and S2; all analytical uncertainties are reported as two-sigma unless otherwise noted.

## 3　Results

The concordia diagrams in Fig. 2 reveal a highly heterogeneous age population, including four concordant Hadean residues with $^{207}Pb/^{206}Pb$ dates ranging from $4142.30 \pm 0.63$ to $4004.20 \pm 0.51$ Ma (excluding tracer and decay constant uncertainty), a wide range of variably discordant L2–L3 leachates, and a distinct, highly discordant population of L1 leachates. Three of the four concordant Hadean zircon residues are derived from a single large grain not previously identified as Hadean, RSES58 z6.10, which also yielded three concordant L3 leachates and a single concordant L2 leachate (all Hadean), as highlighted in Fig. 2c. These concordant ages from different fragments of a single zircon crystal span some 70 Myr. As may be expected from Mattinson (2005) and the success of CA-TIMS over the subsequent decade, leachates are typically more discordant than residues. L1 leachates in particular are markedly more discordant than other analyses, forming a broad array trending towards a lower intercept at the origin (Fig. 2a), as might result from zero-age Pb loss. Four leachate analyses – all of them L2 leachates – yield negatively discordant ages.

Zircon residues are observed in Fig. 3a to be systematically (with only one imprecise exception) older than their respective leachates in $^{207}Pb/^{206}$ space, even at low discordance. For a given zircon fragment, L1–L3 leachates are found to have $^{207}Pb/^{206}Pb$ ages some tens to hundreds of million years younger than residues, with the age gap between corresponding leachates and residues increasing with leachate discordance. In particular, since modern U or Pb re-
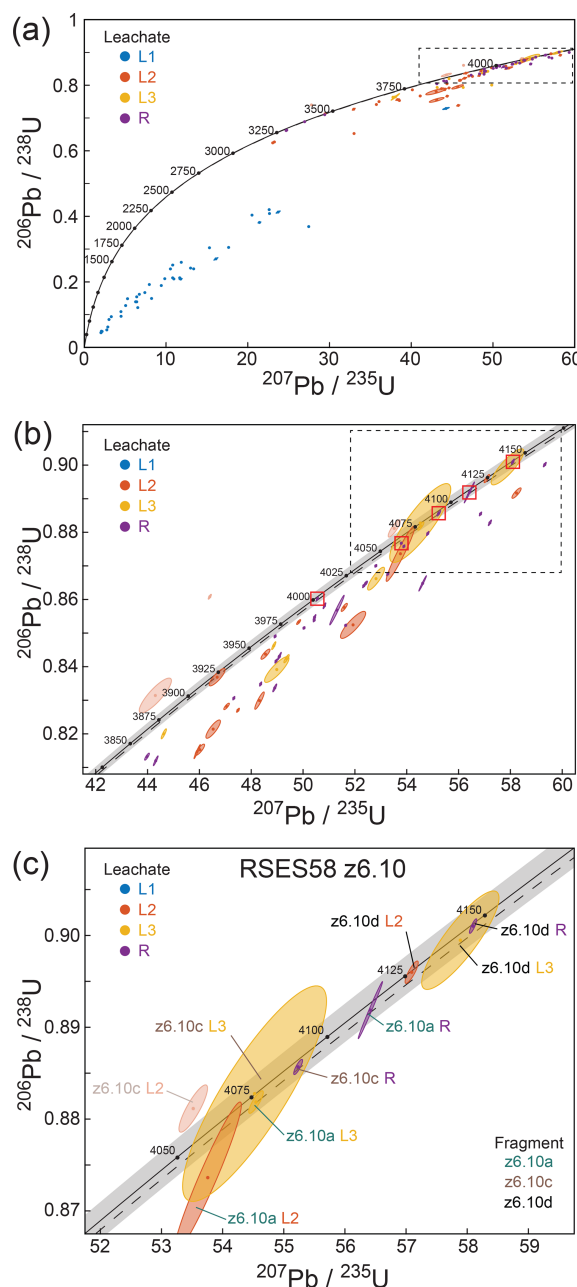


**Figure 2.** CA-ID-TIMS ages for Jack Hills zircon by fragment and leaching step in Wetherill (1956) concordia space. **(a)** Full range, including recent Pb-loss array in L1 leachates. **(b)** Hadean–Eoarchean inset, emphasizing the complexity of the Hadean record and suggesting early lead loss and protracted crystallization history. Concordant residues are highlighted with red squares. **(c)** Concordant fragments and leachates of zircon RSES58 z6.10, illustrating ∼ 50 Myr age heterogeneity between concordant residues of zircon fragments from the same polished half-zircon. At this scale, the uncertainty in the $\lambda_{U-238}/\lambda_{U-235}$ decay constant ratio that defines concordia becomes important; here the solid concordia line and grey two-sigma error envelope reflect the values of Jaffey et al. (1971), while the dashed line reflects those of Schoene et al. (2006). All dates plotted along the concordia line are in millions of years.
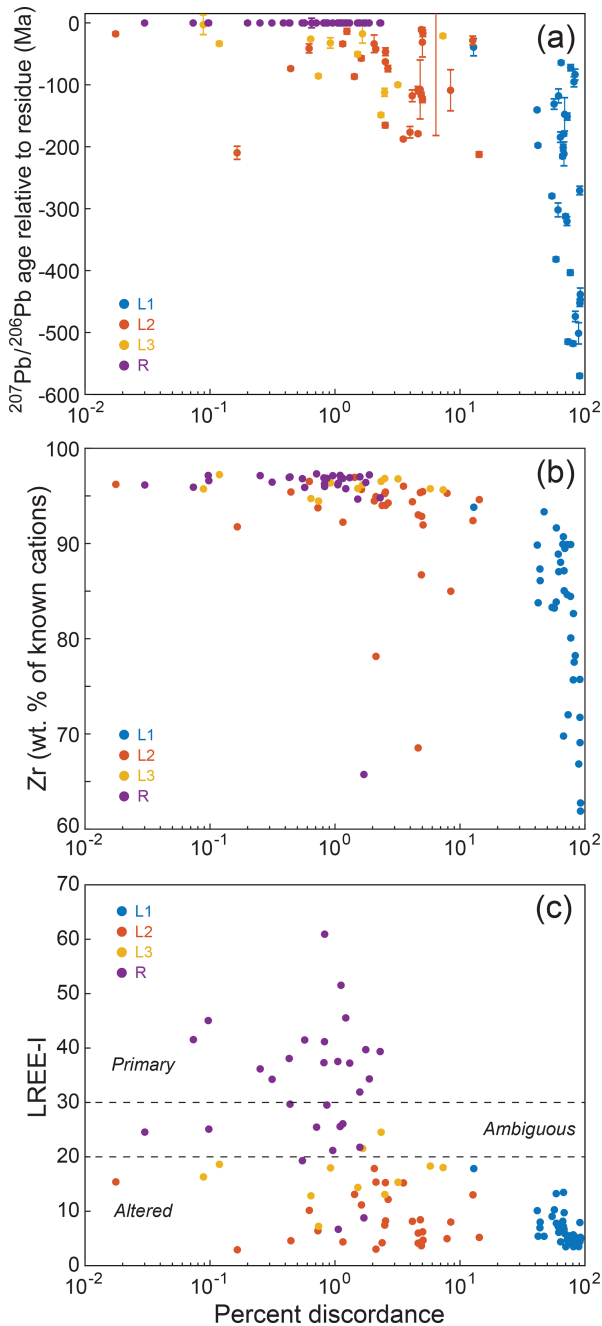
**Figure 3.** **(a)** Age of each leachate relative to its associated residue (if any) plotted as a function of percent discordance. Age offset increases with discordance but may reach $\sim 100$ Myr even for leachates of similar discordance to their residue. **(b)** Abundance of Zr relative to total measured cation concentration as a function of measured discordance. L1 leachates are distinguished by their high discordance and low Zr proportion. **(c)** The light rare earth alteration index (LREE-I $=$ Dy / Nd + Dy / Sm) of Bell et al. (2016, 2019) plotted as a function of measured discordance. High LREE-I in TEA measurements accurately distinguishes primary zircon residues from leachates.

mobilization (e.g., Pb loss without additional isotopic fractionation) has no effect on $^{207}$Pb/$^{206}$Pb ages, systematic age gaps between residues and leachates in $^{207}$Pb/$^{206}$Pb space are most readily attributed to ancient, not recent, Pb loss.

Using the TIMS-TEA methodology of Schoene et al. (2010), we are able to combine trace element and isotopic analyses on the exact same volume of zircon, allowing us to consider the chemical characteristics of zircons that have undergone open-system behavior. We observe that both discordance and leaching extent are strongly correlated with bulk chemistry. In particular, L1 leachates are identifiable by their low Zr content as a proportion of measured cations, as well as their extreme discordance. As observed in Fig. 3b, Zr represents less than 90 % of the measured cation budget by mass in L1 leachate analyses, suggesting that the material removed in L1 leaching steps is not stoichiometric zircon; in later leaching steps, chemistry evolves towards that of the pure zircon residue. Meanwhile, as seen in Fig. 3c, leachates are reliably resolved from pristine residues by the light rare earth index LREE-I of Bell et al. (2016, 2019). Reassuringly, all L1 and L2 leachates fall in the "altered" field defined by Bell et al. (2016) (LREE-I $< 20$), while the "primary" (LREE-I $> 30$) field contains only residues; the remaining analyses fall in the "ambiguous" field of LREE-I for which between 20 and 30 comprise residues and L3 leachates.

On an element-by-element basis, we observe a distinct pattern of trace element enrichment in leachates relative to zircon residues (Fig. 4). L1 leachates display LREE concentrations up to a factor of 25 higher than their corresponding residues, along with smaller enrichments in middle rare earth elements. The discordant L1 leachates are also highly radiogenic, with over 10 times the Pb* of pristine zircon residue. Consistent with Pb loss, this radiogenic lead excess is outpaced by the extreme Th ($\sim 30$ x residue) and U ($\sim 50$ x residue) concentrations of the same leachates. On the same basis, L2 leachates display comparatively muted enrichments in REE, U, Th, and Pb*, while L3 leachates display significant enrichments only in LREE.

A comparison of TIMS and SIMS $^{207}$Pb/$^{206}$Pb ages in Fig. 5 reveals that, for leachates and discordant residues, SIMS ages (typically targeted on low-U cores) are generally older than TIMS ages on fragments of the same grains. Discordant TIMS analyses, especially including early leachates, are likely accessing damaged open-system domains that were excluded from the analyzed SIMS spot. Indeed, depending on the scale of spatial heterogeneity in U–Pb discordance, smaller analytical volumes may be less likely to mix closed- and open-system domains, leading to increased median concordance as a statistical consequence of smaller analytical volume. However, as seen in Fig. 5, TIMS and SIMS $^{207}$Pb/$^{206}$Pb ages are in relatively good agreement for concordant residues surviving the full 12 h of chemical abrasion.
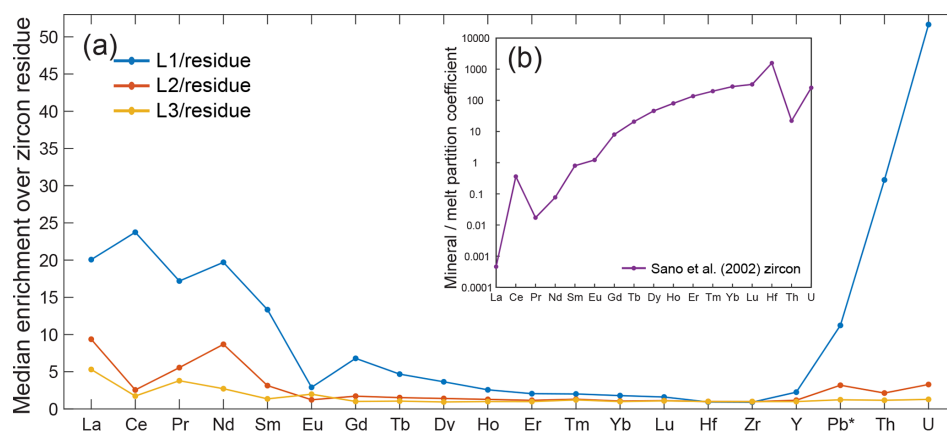
**Figure 4. (a)** Chemical abrasion systematically removes zircon domains rich in LREE, Th, U, and radiogenic Pb. This pattern suggests the preferential removal of zones that have undergone radiation damage and metamiction due to high Th and U content, leaving them vulnerable both to geological open-system behavior (lead loss) and dissolution during chemical abrasion. **(b)** Typical zircon–melt partition coefficients. With the exception of U and Th, the elements that are least abundant in natural zircon display the highest enrichments in L1 leachates: specifically, LREE. However, even a middle rare earth element with positive partition coefficients in crystalline zircon is still enriched in L1 leachates relative to residues. Moreover, the pronounced negative Eu anomaly of L1 leachates suggests a phase with a preference for 3+ over 2+ rare earths. Together, these observations may suggest a role for either (1) coupled substitution in the initial formation of actinide-rich zircon domains or (2) inclusions of rare earth minerals (e.g., monazite, xenotime, or allanite) dissolved during L1 leaching.

## 4 Discussion

### 4.1 Chemical abrasion and U–Pb geochronology

Open-system behavior is arguably the foremost complicating factor in radioisotopic geochronology. With two independent decay chains proceeding at different rates, the U–Pb system in principle allows us to track open-system behavior with discordance and in some cases to even determine the age of Pb loss. Even so, Pb loss when present remains a major limiting factor on the precision and accuracy of inferred primary crystallization ages. For zircon, chemical abrasion has been observed to remove damaged domains that have undergone lead loss and is now widely applied (Mattinson, 2005, 2011; Mundil et al., 2004; Schoene, 2014). However, the same combination of annealing and acid leaching has not been entirely successful in other minerals: monazite responds poorly to annealing (Peterman et al., 2012), while baddeleyite ($ZrO_2$) displays complicated behavior upon abrasion despite its chemical similarity to zircon (Rioux et al., 2010).

Even more puzzling, modern (zero-age) Pb loss is ubiquitous in zircon (Stern et al., 1966; Black, 1987; Hansen and Friderichsen, 1989; Hansen et al., 1989) and to a lesser degree baddeleyite (Reischmann, 1995; Söderlund et al., 2004; Rioux et al., 2010), even when it is not observed in other minerals such as monazite (Black, 1987) and titanite (sphene) (Hansen et al., 1989) from the same sample. Considering the tautological lack of zero-age thermal metamorphism for samples collected at Earth's surface, modern Pb loss does not appear to be a thermal diffusive phenomenon. Further, despite some early suggestions, laboratory handling has been largely ruled out as a source of such zero-age Pb loss (Black, 1987;

much to the contrary, laboratory acid treatment reproducibly decreases normal discordance both in zircon and other minerals (Mattinson, 2005; Rioux et al., 2010; Peterman et al., 2012). Even in unannealed zircon, in which leaching may induce unwanted isotopic fractionation, leachates are consistently more discordant than residues (Mattinson, 1994, 2011; Davis and Krogh, 2001). Clearly, fully understanding these phenomena is central to the reliability of chemically abraded zircon U–Pb ages.

Consistent with literature expectations (Mattinson, 2005, 2011), chemical abrasion is remarkably successful at removing Jack Hills zircon domains that have undergone open-system processes: concordance consistently increases with increasing leaching extent (Figs. 2, 3). Components removed in the first 4 h (L1) are observed to cluster in an array near the origin in Fig. 2, suggesting they have previously undergone near zero-age Pb loss. Chemically, these components are not stoichiometric zircon, with zirconium representing less than 90 % of the cation mass budget. Instead, we suggest that both highly metamict (amorphous) (e.g., Holland and Gottfried, 1955; Utsunomiya et al., 2004) zircons, as well as inclusions and crack-filling precipitates of other less durable minerals, are rapidly dissolved and removed within these first 4 h of chemical abrasion. The geochemistry of material removed during subsequent abrasion steps is markedly closer to that of pristine zircon though still detectably altered according to the LREE-I alteration index of Bell et al. (2016, 2019). These trends mirror the increase in crystalline zircon proportion with increasing leaching extent observed by Widmann et al. (2019).
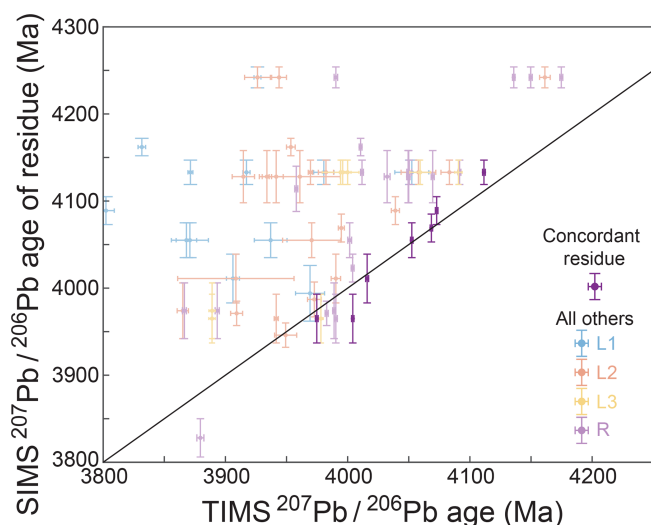
**Figure 5.** Two-variable cross-plot of SIMS spot ages and TIMS $^{207}Pb/^{206}Pb$ ages for each fragment and leachate. Concordant residues (bold) plot along the 1 : 1 line, while others plot above. Horizontal data arrays result from one SIMS spot age per grain plotted against up to four TIMS ages per fragment, with multiple fragments per grain.

To better understand the age of open-system behavior affecting discordant leachate fractions, in Fig. 6a we estimate the vector of Pb loss removed by a single leaching step by plotting discordia arrays defined by sequential analysis pairs for the same fragment. Ordered by leaching step in concordia space, the lower intercept age of Pb loss removed by chemical abrasion steadily increases with leaching extent. In particular, two modes are observed: near zero-age lower intercepts corresponding to L1 leaching steps and broadly Archean lower intercepts corresponding to later leaching steps (Fig. 6b). This trend, along with the relatively pristine zircon chemistry of later leaching steps, may be explained by considering that zircon domains that have undergone ancient but *not* recent lead loss must have been subsequently partially annealed or recrystallized. Such domains would consequently be more resistant to chemical abrasion than their fully metamict counterparts and thus preferentially accessed only in the later stages of chemical abrasion.

These results, in the context of other recent observations, support the conclusion of Black (1987) that zero-age lead loss in zircon results from aqueous processes associated with exposure and incipient weathering. The Jack Hills zircons and their host quartzite have not been affected by any recent tectonothermal disturbances (Spaggiari, 2007a, b), and (according to lithium zonation) have never been metamorphosed above greenschist facies (Trail et al., 2016) – yet they still display pervasive recent and ancient lead loss. In contrast to the terrestrial Jack Hills zircons dated here, lunar zircons of equivalent antiquity display little to no Pb loss even in leachates (Barboni et al., 2017) despite potential exposure to
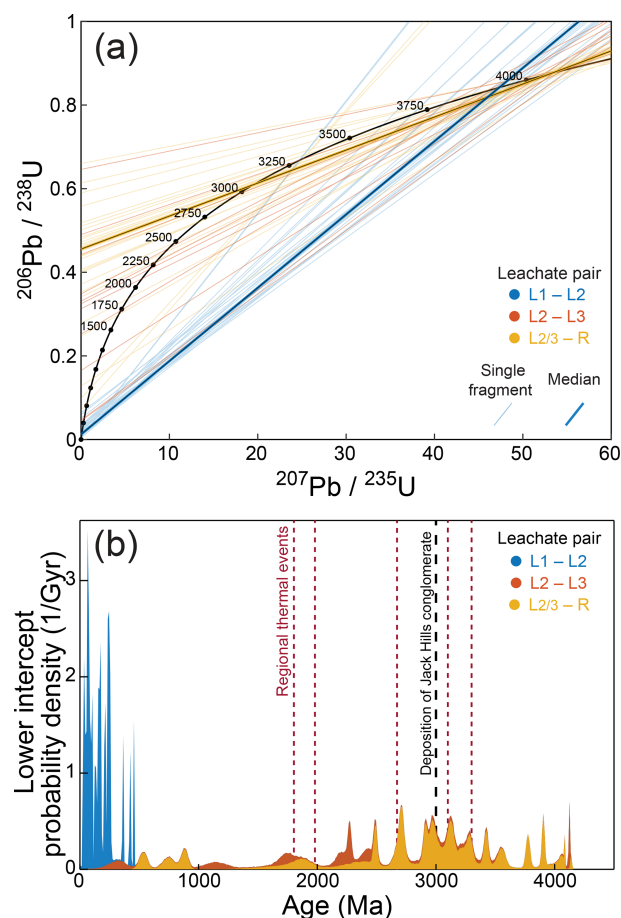


**Figure 6. (a)** Discordia arrays defined by pairs of successive leachate and residue analyses from the same zircon fragment, illustrating the slope and concordia intercepts of each array. **(b)** Probability density plot of the lower intercepts of each leachate-pair discordia array from panel **(a)** with the concordia curve, computed using Monte Carlo methods: repeatedly drawing isotope ratio pairs from the appropriate bivariate normal distributions defining the concordia ellipses for adjacent leachates, calculating the resulting lower intercept each time, and producing a binned histogram of the results. This histogram is plotted along with the nominal dates of known regional thermal events after Spaggiari (2007b) and the approximate depositional age of the Jack Hills metaconglomerate (Spaggiari, 2007a). Arrays defined by L1–L2 leachate pairs have lower intercepts near 0 to 0.5 Ga, while L2-R and (for which three leaching steps were conducted) L3-R pairs define arrays with much older – largely Archean – lower intercepts

shock metamorphism (Crow et al., 2018); one of the clearest distinguishing factors to explain this discrepancy is the near absence of water on the moon.

While diffusion of most cations (including U and Pb) in crystalline zircon is extraordinary slow (Cherniak, 2003), disordered and partially metamict zircon has long been known to be susceptible to aqueous alteration via recrystallization on laboratory timescales at hydrothermal temperatures (Pidgeon et al., 1966; Geisler et al., 2001; Geisler et al.,

2003a, b, 2004) and over longer timescales even at ambient temperatures (Stern et al., 1966; Black, 1987; Tromans, 2006; Delattre et al., 2007). If such aqueous processes are responsible for zero-age Pb loss in zircon, the absence of such Pb loss in monazite and sphene remains notable. While we may consider assigning this discrepancy to factors such as the remarkable resistance of monazite to radiation damage (Seydoux-Guillaume et al., 2018), even fully crystalline monazite and sphene appear susceptible to aqueous recrystallization (Harlov et al., 2010; Gysi et al., 2018). Consequently, we consider the speculative possibility that partial resetting of zircon and baddeleyite during aqueous recrystallization may instead reflect the extreme incompatibility of Pb in the zircon (and baddeleyite) crystal lattice under natural conditions (Watson et al., 1997). In contrast to zircon, sphene displays U/Pb partition coefficient ratios near unity (Tiepolo et al., 2002), while even monazite, with a mineral–melt Pb partition coefficient likely less than 0.1 (Stepanov et al., 2012), has been observed to incorporate significant $Pb_c$ (Seydoux-Guillaume et al., 2003; Fougerouse et al., 2018): up to 80 % of total Pb in hydrothermally altered monazite (Seydoux-Guillaume et al., 2012; Didier et al., 2013). In this context the comparative immunity of higher-$Pb_c$ minerals like monazite and sphene to such exposure-related resetting may represent closed-system aqueous recrystallization enabled by their comparatively higher tolerance for Pb substitution.

Why, then, does chemical abrasion succeed for zircon but not baddeleyite? While a full discussion is beyond the scope of this paper, we may note one possibility. When heated above $\sim 800\,^{\circ}\mathrm{C}$ at atmospheric pressure, metamict zircon decomposes into microcrystalline $ZrO_2$ and $SiO_2$, the latter of which is partially volatilized (Nasdala et al., 2002; Váczi et al., 2009). This process is evidently sensitive to the crystallinity and surface area of the zircon in question and forms the basis for the whole-grain direct evaporation technique of Kober (1986). Since the products of the low-temperature aqueous recrystallization of metamict zircon appear to remain rather poorly crystalline (featuring microlites, nanopores, and residual amorphous zones; Geisler et al., 2003b, 2004; Delattre et al., 2007; Hay et al., 2009), partially metamict zircon that has undergone exposure-associated aqueous Pb loss and recrystallization should remain susceptible to oxide decomposition during low-pressure, high-temperature annealing. If this interpretation is correct, the high temperature at which this conversion occurs (limiting isotopic fractionation), followed by quantitative dissolution of highly acid-soluble (Rioux et al., 2010) $ZrO_2$ crystallites during chemical abrasion, may explain why isotopic fractionation and reverse discordance are rare in the chemical abrasion of annealed zircon.

## 4.2 Geological history of Hadean Jack Hills zircons

Despite the limited metamorphic grade of the Jack Hills conglomerate (Spaggiari, 2007a, b; Trail et al., 2016), All zircon fragments we analyzed show clear chemical signs of alteration in leachate fractions, with enrichments in LREE, U, and Th corresponding to low LREE-I in the altered field of Bell et al. (2016, 2019). In L1 leachates, which also display relatively low Zr cation proportions, the extreme enrichments in LREE, U, and Th may be attributed in part to inclusions or crack-filling secondary minerals. The more modest enrichments in L2 and L3 leachates are more likely attributable to partially metamict zircon. This latter case leads unavoidably to some ambiguity regarding the origin of the atypical chemistry of these leachates: if certain zones in a given zircon are preferentially metamict, they must have crystallized with particularly high U and Th concentrations. However, since magmatic zircon has not been observed to crystallize with high LREE, we may assume these contaminants were added at or near the time that Pb was lost from the metamict source domains of L2 and L3 leachates. Fortunately, the two independent decay chains of the U–Pb system allow us to estimate the timing of this alteration.

While highly heterogeneous, the lower intercepts of leachate pairs may be crudely divided between two modes: one modern and one Archean (Fig. 6). The complete decoupling of the major L1–L2 Pb-loss mode from any known regional metamorphic events in the Narryer terrane is consistent with the hypothesis that this represents aqueous recrystallization during modern exposure and weathering. In this context, it may be significant that the lower intercepts of L2/3–R pairs broadly scatter around the estimated depositional age of the Jack Hills quartzite, with a mean lower intercept of 3050 Ma.

While the discordia arrays defined by successive leaching steps are subject to substantial interpretive uncertainty (and need not be geologically meaningful considering the possibility of time-transgressive Pb loss), it is nonetheless apparent from Fig. 6 that L2 and L3 domains do not appear to have been heavily influenced by the same zero-age Pb-loss process seen in L1 domains, suggesting that such domains are not as damaged as they once were. Consequently, it appears that either ancient low-grade metamorphic events or prolonged burial may have acted to partially anneal these domains, locking in ancient Pb loss. In other words, regional metamorphic events in the Narryer terrane appear, if anything, to halt – not initiate – Pb loss. Subaerial exposure and aqueous weathering – not metamorphism – may explain modern and ancient open-system behavior in the Jack Hills zircons. Such a model parsimoniously reconciles the complicated multiple-Pb-loss history of the Jack Hills zircons (e.g., Fig. 2) with their relative lack (Trail et al., 2016) of high-grade metamorphism.

Finally, concordant Jack Hills zircon residues that have survived chemical abrasion still display dramatic age heterogeneity, with a 50 Myr range observed between differ-

ent fragments of the same zircon, as seen in Fig. 2c. While chemical abrasion may imperfectly or incompletely remove domains that have undergone ancient open-system behavior, any modern U or Pb loss or addition would occur along a markedly steeper line in $^{206}Pb/^{238}U$–$^{207}Pb/^{235}U$ space and thus cannot explain the observed age heterogeneity in RSES58 z6.10. Nonetheless, due to the minimal curvature of concordia over this age range, we cannot rule out early ($> 4$ Ga) open-system behavior as a cause of this dispersion, even with ID-TIMS precision on the $< 0.05$ % level. Considering the infeasibility of high-temperature diffusive daughter loss without dissolution and recrystallization below zircon saturation temperature (Cherniak et al., 1997; Cherniak, 2003; Boehnke et al., 2013; Keller et al., 2017), we are left with two end-member scenarios to explain the observed age heterogeneity in RSES58 z6.10: (1) high-temperature overgrowth and (2) low-temperature recrystallization. The former suggests repeated magmatic or orogenic events within the Hadean; the latter likely requires the presence of liquid water.

## 5  Conclusions

Stepwise CA-ID-TIMS-TEA confirms the Hadean SIMS ages of Jack Hills zircon fragments, while providing insight into both the geological history of open-system behavior in the Jack Hills zircons and the operation and effectiveness of the zircon chemical abrasion procedure of Mattinson (2005). Jack Hills zircon residues and leachates exhibit complex discordance, suggesting at least two recorded modes of post-Hadean Pb loss, as well as at least one episode of Hadean recrystallization or overgrowth. Concordant Hadean residues reveal 50 Myr of age heterogeneity in the fragments of RSES 58 z6.10, suggesting this single zircon may have experienced multiple episodes of magmatism within the Hadean.

Most Pb loss in the Hadean Jack Hills zircons studied here substantially postdates the Hadean, with episodes focused around $\sim 0$ and $\sim 3$ Ga, potentially ameliorating some concerns about the impact of Pb loss on the Hadean hafnium isotope record. Moreover, such Pb loss does not appear to be driven by high-temperature metamorphism; on the contrary, regional metamorphic events of the Narryer terrane appear to correlate with the partial annealing of ancient radiation damage, halting and locking in evidence of ancient Pb loss in the L3 and L2 – but not L1 – domains. Instead, following Stern et al. (1966) and Black (1987), we propose that Pb loss in metamict zircon domains is frequently a result of low-temperature aqueous recrystallization associated with weathering and subaerial exposure.

While small-scale aqueous recrystallization might well be envisioned as a closed-system process for many minerals, we further propose that the extreme incompatibility of Pb in zircon and baddeleyite ensures that Pb is excluded during aqueous recrystallization. Hence, zero-age Pb loss is apparent in zircon and baddeleyite even when it is absent in, e.g., co-existing sphene or monazite. Considering the central role of water in this mechanism of Pb loss, this hypothesis may explain the ubiquity of recent Pb loss in terrestrial – but not lunar – zircon.

Our isotopic and trace element results are consistent with the prior expectation that chemical abrasion (Mattinson, 2005) effectively removes zircon domains that have undergone partial open-system behavior, including both metamict zircon and contaminating inclusions. Over the course of 12 h of HF leaching, leachate chemistry evolves from U-, Th-, and LREE-enriched towards normal zircon and from discordant to concordant, mirroring the increase in crystallinity observed by Widmann et al. (2019). While the first (L1) leachates are the most radiogenic, they are also the most discordant and reflect the youngest Pb loss (Fig. 6). The cation proportion of Zr is diminished only in L1 leachates, suggesting most inclusions are removed in the first 4 h of chemical abrasion. Meanwhile, elevated U and Th contents in leachates are consistent with the hypothesis that chemical abrasion preferentially removes the same metamict domains that are susceptible to Pb loss through aqueous recrystallization.

Finally, we find that the LREE-I alteration index of Bell et al. (2016, 2019) accurately identifies non-primary geochemistry in discordant leachates. In particular, these results demonstrate that the trace element ratio cutoffs defined by Bell et al. (2016) to identify alteration via SIMS are also applicable to trace element concentrations determined by ICPMS in the TIMS-TEA (Schoene et al., 2010) workflow. Consequently, we hypothesize that screening in situ analyses by LREE-I on a cycle-by-cycle basis (with, e.g., split stream techniques) may allow in situ U–Pb analyses to reject the same altered domains that are removed by chemical abrasion in CA-TIMS.

# References

Amelin, Y., Lee, D.-C., Halliday, A. N., and Pidgeon, R. T.: Nature of the Earth's earliest crust from hafnium isotopes in single detrital zircons, Nature, 399, 252–255, 1999.

Amelin, Y. V.: Geochronology of the Jack hills detrital zircons by precise U-Pb isotope dilution analysis of crystal fragments, Chem. Geol., 146, 25–38, 1998.

Barboni, M., Boehnke, P., Keller, C. B., Kohl, I. E., Schoene, B., Young, E. D., and McKeegan, K. D.: Early formation of the Moon 4.51 billion years ago, Sci. Adv., 3, e1602365, https://doi.org/10.1126/sciadv.1602365, 2017.

Bédard, J. H.: Stagnant lids and mantle overturns: Implications for Archaean tectonics, magmagenesis, crustal growth, mantle evolution, and the start of plate tectonics, Geosci. Front., 9, 19–49, 2018.

Bell, E. A., Harrison, T. M., Kohl, I. E., and Young, E. D.: Eoarchean crustal evolution of the Jack Hills zircon source and loss of Hadean crust, Geochim. Cosmochim. Acta, 146, 27–42, 2014.

Bell, E. A., Boehnke, P., Hopkins-Wielicki, M. D., and Harrison, T. M.: Distinguishing primary and secondary inclusion assemblages in Jack Hills zircons, Lithos, 234–235, 15–26, 2015.

Bell, E. A., Boehnke, P., and Harrison, T. M.: Recovering the primary geochemistry of Jack Hills zircons through quantitative estimates of chemical alteration, Geochim. Cosmochim. Acta, 191, 187–202, 2016.

Bell, E. A., Boehnke, P., Barboni, M., and Harrison, T. M.: Tracking chemical alteration in magmatic zircon using rare earth element abundances, Chem. Geol., 510, 56–71, 2019.

Black, L. P.: Recent Pb loss in zircon: A natural or laboratory-induced phenomenon?, Chem. Geol. Isotope Geoscience section, 65, 25–33, 1987.

Boehnke, P., Watson, E. B., Trail, D., Harrison, T. M., and Schmitt, A. K.: Zircon saturation re-revisited, Chem. Geol., 351, 324–334, 2013.

Bowring, J. F. and McLean, N. M.: Engineering cyber infrastructure for U-Pb geochronology: Tripoli and U-Pb Redux, Geochem. Geophys. Geosyst., 12, 1–19, 2011.

Bowring, S. A. and Williams, I. S.: Priscoan (4.00–4.03 Ga) orthogneisses from northwestern Canada, Contrib. Mineral. Petrol., 134, 3–16, 1999.

Byerly, B. L., Lowe, D. R., Drabon, N., Coble, M. A., Burns, D. H., and Byerly, G. R.: Hadean zircon from a 3.3 Ga sandstone, Barberton Greenstone Belt, South Africa, Geology, 46, 967–970, 2018.

Cavosie, A. J., Valley, J. W., Wilde, S. A., and E. I. M. F.: Magmatic $\delta^{18}O$ in 4400–3900 Ma detrital zircons: A record of the alteration and recycling of crust in the Early Archean, Earth Planet. Sci. Lett., 235, 663–681, 2005.

Cavosie, A. J., Valley, J. W., and Wilde, S. A.: The oldest terrestrial mineral record: A review of 4400 to 4000 Ma detrital zircons from Jack Hills, Western Australia, in: Earths Oldest Rocks, 91–111, Elsevier, 2007.

Cherniak, D. J.: Diffusion in Zircon, Rev. Mineral. Geochem., 53, 113–143, 2003.

Cherniak, D. J., Hanchar, J. M., and Watson, E. B.: Diffusion of tetravalent cations in zircon, Contrib. Mineral. Petrol., 127, 383–390, 1997.

Compston, W. and Pidgeon, R. T.: Jack Hills, evidence of more very old detrital zircons in Western Australia, Nature, 321, 766–769, 1986.

Condie, K. C.: A planet in transition: The onset of plate tectonics on Earth between 3 and 2 Ga?, Geosci. Front., 9, 51–60, 2018.

Condon, D. J., Schoene, B., McLean, N. M., Bowring, S. A., and Parrish, R. R.: Metrology and traceability of U-Pb isotope dilution geochronology (EARTHTIME Tracer Calibration Part I), Geochim. Cosmochim. Acta, 164, 464–480, 2015.

Crow, C. A., Moser, D. E., and McKeegan, K. D.: Shock metamorphic history of > 4 Ga Apollo 14 and 15 zircons, Meteor. Planet. Sci., 54, 181–201, https://doi.org/10.1111/maps.13184 if needed, 2018.

Davis, D. W. and Krogh, T. E.: Preferential dissolution of $^{234}$U and radiogenic Pb from $\alpha$-recoil-damaged lattice sites in zircon: implications for thermal histories and Pb isotopic fractionation in the near surface environment, Chem. Geol., 172, 41–58, 2001.

Delattre, S., Utsunomiya, S., Ewing, R. C., Boeglin, J.-L., Braun, J.-J., Balan, E., and Calas, G.: Dissolution of radiation-damaged zircon in lateritic soils, Am. Mineral., 92, 1978–1989, 2007.

Didier, A., Bosse, V., Boulvais, P., Bouloton, J., Paquette, J.-L., Montel, J. M., and Devidal, J. L.: Disturbance versus preservation of U-Th-Pb ages in monazite during fluid-rock interaction: textural, chemical and isotopic in situ study in microgranites (Velay Dome, France), Contrib. Mineral. Petrol., 165, 1051–1072, 2013.

Duo, J., Wen, C., Guo, J., Fan, X., and Li, X.: 4.1 Ga old detrital zircon in western Tibet of China, Chi. Sci. Bull., 52, 23–26, 2007.

Fougerouse, D., Reddy, S. M., Saxey, D. W., Erickson, T. M., Kirkland, C. L., Rickard, W. D. A., Seydoux-Guillaume, A. M., Clark, C., and Buick, I. S.: Nanoscale distribution of Pb in monazite revealed by atom probe microscopy, Chem. Geol., 479, 251–258, 2018.

Froude, D. O., Ireland, T. R., Kinny, P. D., Williams, I. S., Compston, W., Williams, I. R., and Myers, J. S.: Ion microprobe identification of 4,100–4,200 Myr-old terrestrial zircons, Nature, 304, 616, 1983.

Geisler, T., Ulonska, M., Schleicher, H., Pidgeon, R. T., and van Bronswijk, W.: Leaching and differential recrystallization of metamict zircon under experimental hydrothermal conditions, Contrib. Mineral. Petrol., 141, 53–65, 2001.

Geisler, T., Pidgeon, R. T., Kurtz, R., van Bronswijk, W., and Schleicher, H.: Experimental hydrothermal alteration of partially metamict zircon, Am. Mineral., 88, 1496–1513, 2003a.

Geisler, T., Zhang, M., and Salje, E. K. H.: Recrystallization of almost fully amorphous zircon under hydrothermal conditions:

An infrared spectroscopic study, J. Nuc. Mater., 320, 280–291, 2003b.

Geisler, T., Seydoux-Guillaume, A.-M., Wiedenbeck, M., Wirth, R., Berndt, J., Zhang, M., Mihailova, B., Putnis, A., Salje, E. K. H., and Schlüter, J.: Periodic precipitation pattern formation in hydrothermally treated metamict zircon, Am. Mineral., 89, 1341–1347, 2004.

Gerstenberger, H. and Haase, G.: A highly effective emitter substance for mass spectrometric Pb isotope ratio determinations, Chem. Geol., 136, 309–312, 1997.

Guitreau, M. and Blichert-Toft, J.: Implications of discordant U-Pb ages on Hf isotope studies of detrital zircons, Chem. Geol., 385, 17–25, 2014.

Gysi, A. P., Harlov, D., and Miron, G. D.: The solubility of monazite ($CePO_4$), $SmPO_4$, and $GdPO_4$ in aqueous solutions from 100 to 250 C, Geochim. Cosmochim. Acta, 242, 143–164, 2018.

Hansen, B. T. and Friderichsen, J. D.: The influence of recent lead loss on the interpretation of disturbed U-Pb systems in zircons from igneous rocks in East Greenland, Lithos, 23, 209–223, 1989.

Hansen, B. T., Persson, P. O., Söllner, F., and Lindh, A.: The influence of recent lead loss on the interpretation of disturbed U-Pb systems in zircons from metamorphic rocks in southwest Sweden, Lithos, 23, 123–136, 1989.

Harlov, D. E., Wirth, R., and Hetherington, C. J.: Fluid-mediated partial alteration in monazite: the role of coupled dissolution-reprecipitation in element redistribution and mass transfer, Contrib. Mineral. Petrol., 162, 329–348, 2010.

Harrison, T. M.: The Hadean crust: Evidence from 4 Ga zircons, Ann. Rev. Earth Planet. Sci., 37, 479–505, 2009.

Harrison, T. M., Bell, E. A., and Boehnke, P.: Hadean Zircon Petrochronology, Rev. Mineral. Geochem., 83, 329–363, 2017.

Hay, D. C., Dempster, T. J., Lee, M. R., and Brown, D. J.: Anatomy of a low temperature zircon outgrowth, Contrib. Mineral. Petrol., 159, 81–92, 2009.

Hiess, J., Condon, D. J., McLean, N. M., and Noble, S. R.: $^{238}U/^{235}U$ Systematics in terrestrial uranium-bearing minerals, Science, 335, 1610–1614, 2012.

Holden, P., Lanc, P., Ireland, T. R., Harrison, T. M., Foster, J. J., and Bruce, Z.: Mass-spectrometric mining of Hadean zircons by automated SHRIMP multi-collector and single-collector U/Pb zircon age dating: The first 100,000 grains, Int. J. Mass Spectrom., 286, 53–63, 2009.

Holland, H. D. and Gottfried, D.: The effect of nuclear radiation on the structure of zircon, Acta Crystall., 8, 291–300, 1955.

Hopkins, M. D., Harrison, T. M., and Manning, C. E.: Constraints on Hadean geodynamics from mineral inclusions in > 4 Ga zircons, Earth Planet. Sci. Lett., 298, 367–376, 2010.

Hoskin, P. W. O. and Schaltegger, U.: The composition of zircon and igneous and metamorphic petrogenesis, Rev. Mineral. Geochem., 53, 27–62, 2003.

Iizuka, T., Horie, K., Komiya, T., Maruyama, S., Hirata, T., Hidaka, H., and Windley, B. F.: 4.2 Ga zircon xenocryst in an Acasta gneiss from northwestern Canada: Evidence for early continental crust, Geology, 34, 245–248, 2006.

Jaffey, A. H., Flynn, K. F., Glendenin, L. E., and Bentley, W. C.: Precision Measurement of Half-Lives and Specific Activities of $^{235}U$ and $^{238}U$, Phys. Rev. C, 4, 1889–1906, 1971.

Keller, C. B. and Schoene, B.: Plate tectonics and continental basaltic geochemistry throughout Earth history, Earth Planet. Sci. Lett., 481, 290–304, 2018.

Keller, C. B., Boehnke, P., and Schoene, B.: Temporal variation in relative zircon abundance throughout Earth history, Geochem. Persp. Lett., 3, 179–189, 2017.

Keller, C. B., Boehnke, P., Schoene, B., and Harrison, T. M.: Stepwise chemical abrasion ID-TIMS-TEA of microfractured Hadean zircon, OSF Home, https://doi.org/10.17605/OSF.IO/AVDQH, 2019.

Kelly, N. M. and Harley, S. L.: An integrated microtextural and chemical approach to zircon geochronology: refining the Archaean history of the Napier Complex, east Antarctica, Contrib. Mineral. Petrol., 149, 57–84, 2005.

Kober, B.: Whole-grain evaporation for $^{207}Pb/^{206}Pb$-age-investigations on single zircons using a double-filament thermal ion source, Contrib. Mineral. Petrol., 93, 482–490, 1986.

Krogh, T. E.: A low-contamination method for hydrothermal decomposition of zircon and extraction of U and Pb for isotopic age determinations, Geochim. Cosmochim. Acta, 37, 485–494, 1973.

Kusiak, M. A., Whitehouse, M. J., Wilde, S. A., Dunkley, D. J., Menneken, M., Nemchin, A. A., and Clark, C.: Changes in zircon chemistry during Archean UHT metamorphism in the Napier Complex, Antarctica, Am. J. Sci., 313, 933–967, 2013.

Maas, R., Kinny, P. D., Williams, I. S., Froude, D. O., and Compston, W.: The Earth's oldest known crust: A geochronological and geochemical study of 3900–4200 Ma old detrital zircons from Mt. Narryer and Jack Hills, Western Australia, Geochim. Cosmochim. Acta, 56, 1281–1300, 1992.

Mattinson, J. M.: A study of complex discordance in zircons using step-wise dissolution techniques, Contrib. Mineral. Petrol., 116, 117–129, 1994.

Mattinson, J. M.: Zircon U-Pb chemical abrasion ("CA-TIMS") method: Combined annealing and multi-step partial dissolution analysis for improved precision and accuracy of zircon ages, Chem. Geol., 220, 47–66, 2005.

Mattinson, J. M.: Extending the Krogh legacy: development of the CA-TIMS method for zircon U-Pb geochronologyThis article is one of a series of papers published in this Special Issue on the theme of Geochronology in honour of Tom Krogh, Can. J. Earth Sci., 48, 95–105, 2011.

McLean, N. M., Bowring, J. F., and Bowring, S. A.: An algorithm for U-Pb isotope dilution data reduction and uncertainty propagation, Geochem. Geophys. Geosyst., 12, 1–12, 2011.

McLean, N. M., Condon, D. J., Schoene, B., and Bowring, S. A.: Evaluating uncertainties in the calibration of isotopic reference materials and multi-element isotopic tracers (EARTHTIME Tracer Calibration Part II), Geochim. Cosmochim. Acta, 164, 481–501, 2015.

Miller, S. R., Mueller, P. A., Meert, J. G., Kamenov, G. D., Pivarunas, A. F., Sinha, A. K., and Pandit, M. K.: Detrital zircons reveal evidence of Hadean crust in the Singhbhum Craton, India, The J. Geol., 126, 541–552, 2018.

Mojzsis, S. J. and Harrison, T. M.: Establishment of a 3.83-Ga magmatic age for the Akilia tonalite (southern West Greenland), Earth Planet. Sci. Lett., 202, 563–576, 2002.

Mojzsis, S. J., Harrison, T. M., and Pidgeon, R. T.: Oxygen-isotope evidence from ancient zircons for liquid water at the Earth's surface 4,300 Myr ago, Nature, 409, 178–181, 2001.

Mundil, R., Ludwig, K. R., Metcalfe, I., and Renne, P. R.: Age and timing of the Permian mass extinctions: U/Pb dating of closed-system zircons, Science, 305, 1760–1763, 2004.

Myers, J. S.: Early Archaean Narryer Gneiss Complex, Yilgarn Craton, Western Australia, Precamb. Res., 38, 297–307, 1988.

Nadeau, S., Chen, W., Reece, J., Lachhman, D., Ault, R., Faraco, M. T. L., Fraga, L. M., Reis, N. J., and Betiollo, L. M.: Guyana: the lost Hadean crust of South America?, Braz. J. Geol., 43, 601–606, 2013.

Nasdala, L., Lengauer, C. L., Hanchar, J. M., Kronz, A., Wirth, R., Blanc, P., Kennedy, A. K., and Seydoux-Guillaume, A.-M.: Annealing radiation damage and the recovery of cathodoluminescence, Chem. Geol., 191, 121–140, 2002.

Paquette, J.-L., Barbosa, J. S. F., Rohais, S., Cruz, S. C. P., Goncalves, P., Peucat, J. J., Leal, A. B. M., Santos-Pinto, M., and Martin, H.: The geological roots of South America: 4.1 Ga and 3.7 Ga zircon crystals discovered in N.E. Brazil and N.W. Argentina, Precamb. Res., 271, 49–55, 2015.

Peterman, E. M., Mattinson, J. M., and Hacker, B. R.: Multi-step TIMS and CA-TIMS monazite U-Pb geochronology, Chem. Geol., 312–313, 58–73, 2012.

Pidgeon, R. T., O'Neil, J. R., and Silver, L. T.: Uranium and lead isotopic stability in a metamict zircon under experimental hydrothermal conditions, Science, 154, 1538–1540, 1966.

Reischmann, T.: Precise U/Pb age determination with baddeleyite ($ZrO_2$), a case study from the Phalaborwa igneous complex, South Africa, South Afr. J. Geol., 98, 1–4, 1995.

Rioux, M., Bowring, S., Dudás, F., and Hanson, R.: Characterizing the U-Pb systematics of baddeleyite through chemical abrasion: application of multi-step digestion methods to baddeleyite geochronology, Contrib. Mineral. Petrol., 160, 777–801, 2010.

Schoene, B.: U-Th-Pb Geochronology, in: Treatise on Geochemistry, edited by: Rudnick, R. L., 341–378, Elsevier, 2014.

Schoene, B., Crowley, J. L., Condon, D. J., Schmitz, M. D., and Bowring, S. A.: Reassessing the uranium decay constants for geochronology using ID-TIMS U-Pb data, Geochim. Cosmochim. Acta, 70, 426–445, 2006.

Schoene, B., Latkoczy, C., Schaltegger, U., and Günther, D.: A new method integrating high-precision U-Pb geochronology with zircon trace element analysis (U-Pb TIMS-TEA), Geochimica et Cosmochimica Acta, 74, 7144–7159, 2010.

Schoene, B., Samperton, K. M., Eddy, M. P., Keller, G., Adatte, T., Bowring, S. A., Khadri, S. F. R., and Gertsch, B.: U-Pb geochronology of the Deccan Traps and relation to the end-Cretaceous mass extinction, Science, 347, 182–184, 2015.

Seydoux-Guillaume, A.-M., Goncalves, P., Wirth, R., and Deutsch, A.: Transmission electron microscope study of polyphase and discordant monazites: Site-specific specimen preparation using the focused ion beam technique, Geology, 31, 973, 2003.

Seydoux-Guillaume, A.-M., Montel, J.-M., Bingen, B., Bosse, V., de Parseval, P., Paquette, J.-L., Janots, E., and Wirth, R.: Low-temperature alteration of monazite: Fluid mediated coupled dissolution–precipitation, irradiation damage, and disturbance of the U-Pb and Th-Pb chronometers, Chem. Geol., 330–331, 140–158, 2012.

Seydoux-Guillaume, A.-M., Deschanels, X., Baumier, C., Neumeier, S., Weber, W. J., and Peuget, S.: Why natural monazite never becomes amorphous: Experimental evidence for alpha self-healing, Am. Mineral., 103, 824–827, 2018.

Söderlund, U., Patchett, P. J., Vervoort, J. D., and Isachsen, C. E.: The $^{176}Lu$ decay constant determined by Lu-Hf and U-Pb isotope systematics of Precambrian mafic intrusions, Earth Planet. Sci. Lett., 219, 311–324, 2004.

Spaggiari, C. V.: The Jack Hills greenstone belt, Western Australia: Part 2: Lithological relationships and implications for the deposition of $\geq 4.0$ Ga detrital zircons, Precamb. Res., 155, 261–286, 2007a.

Spaggiari, C. V.: The Jack Hills greenstone belt, Western Australia: Part 1: Structural and tectonic evolution over > 1.5 Ga, Precamb. Res., 155, 204–228, 2007b.

Stepanov, A. S., Hermann, J., Rubatto, D., and Rapp, R. P.: Experimental study of monazite/melt partitioning with implications for the REE, Th and U geochemistry of crustal rocks, Chem. Geol., 300–301, 200–220, 2012.

Stern, T. W., Goldich, S. S., and Newell, M. F.: Effects of weathering on the U-Pb ages of zircon from the Morton Gneiss, Minnesota, 1, 369–371, 1966.

Tiepolo, M., Oberti, R., and Vannucci, R.: Trace-element incorporation in titanite: constraints from experimentally determined solid/liquid partition coefficients, Chem. Geol., 191, 105–119, 2002.

Trail, D., Mojzsis, S. J., Harrison, T. M., Schmitt, A. K., Watson, E. B., and Young, E. D.: Constraints on Hadean zircon protoliths from oxygen isotopes, Ti-thermometry, and rare earth elements, Geochem. Geophys. Geosyst., 8, 1–22, 2007.

Trail, D., Watson, E. B., and Tailby, N. D.: The oxidation state of Hadean magmas and implications for early Earth's atmosphere, Nature, 480, 79–82, 2011.

Trail, D., Cherniak, D. J., Watson, E. B., Harrison, T. M., Weiss, B. P., and Szumila, I.: Li zoning in zircon as a potential geospeedometer and peak temperature indicator, Contrib. Mineral. Petrol., 171, 1–15, 2016.

Tromans, D.: Solubility of crystalline and metamict zircon: A thermodynamic analysis, J. Nuclear Mater., 357, 221–233, 2006.

Utsunomiya, S., Palenik, C. S., Valley, J. W., Cavosie, A. J., Wilde, S. A., and Ewing, R. C.: Nanoscale occurrence of Pb in an Archean zircon, Geochim. Cosmochim. Acta, 68, 4679–4686, 2004.

Váczi, T., Nasdala, L., Wirth, R., Mehofer, M., Libowitzky, E., and Häger, T.: On the breakdown of zircon upon "dry" thermal annealing, Mineral. Petrol., 97, 129–138, 2009.

Valley, J. W., Cavosie, A. J., Ushikubo, T., and Reinhard, D. A.: Hadean age for a post-magma-ocean zircon confirmed by atom-probe tomography, Nat. Geosci., 7, 219–223, 2014.

Wang, H., Chen, L., Sun, Y., Liu, X., Xu, X., Chen, J., Zhang, H., and Diwu, C.: 4.1 Ga xenocrystal zircon from Ordovician volcanic rocks in western part of North Qinling Orogenic Belt, Chi. Sci. Bull., 52, 3002–3010, 2007.

Watson, E. B.: Zircon Thermometer Reveals Minimum Melting Conditions on Earliest Earth, Science, 308, 841–844, 2005.

Watson, E. B., Chemiak, D. J., Hanchar, J. M., Harrison, T. M., and Wark, D. A.: The incorporation of Pb into zircon, Chem. Geol., 141, 19–31, 1997.

Wetherill, G. W.: Discordant uranium-lead ages, I, Trans. Am. Geophys. Union, 37, 320–326, 1956.

Whitehouse, M. J., Nemchin, A. A., and Pidgeon, R. T.: What can Hadean detrital zircon really tell us? A critical evaluation of their geochronology with implications for the interpretation of oxygen and hafnium isotopes, Gondwana Res., 51, 78–91, 2017.

Widmann, P., Davies, J. H. F. L., and Schaltegger, U.: Calibrating chemical abrasion: Its effects on zircon crystal structure, chemical composition and UPb age, Chem. Geol., 511, 1–10, 2019.

Wilde, S. A., Valley, J. W., Peck, W. H., and Graham, C. M.: Evidence from detrital zircons for the existence of continental crust and oceans on the Earth 4.4 Gyr ago, Nature, 409, 175–178, 2001.

Xing, G.-F., Wang, X.-L., Wan, Y., Chen, Z.-H., Jiang, Y., Kitajima, K., Ushikubo, T., and Gopon, P.: Diversity in early crustal evolution: 4100 Ma zircons in the Cathaysia Block of southern China, Sci. Rep., 4, 5143, 2014.

Xu, Y., Du, Y., Huang, H., Huang, Z., Hu, L., Zhu, Y., and Yu, W.: Detrital zircon of 4.1 Ga in South China, Chi. Sci. Bull., 57, 4356–4362, 2012.

*Supplement of*

# Stepwise chemical abrasion–isotope dilution–thermal ionization mass spectrometry with trace element analysis of microfractured Hadean zircon

**C. Brenhin Keller et al.**

*Correspondence to:* C. Brenhin Keller (cbkeller@dartmouth.edu)
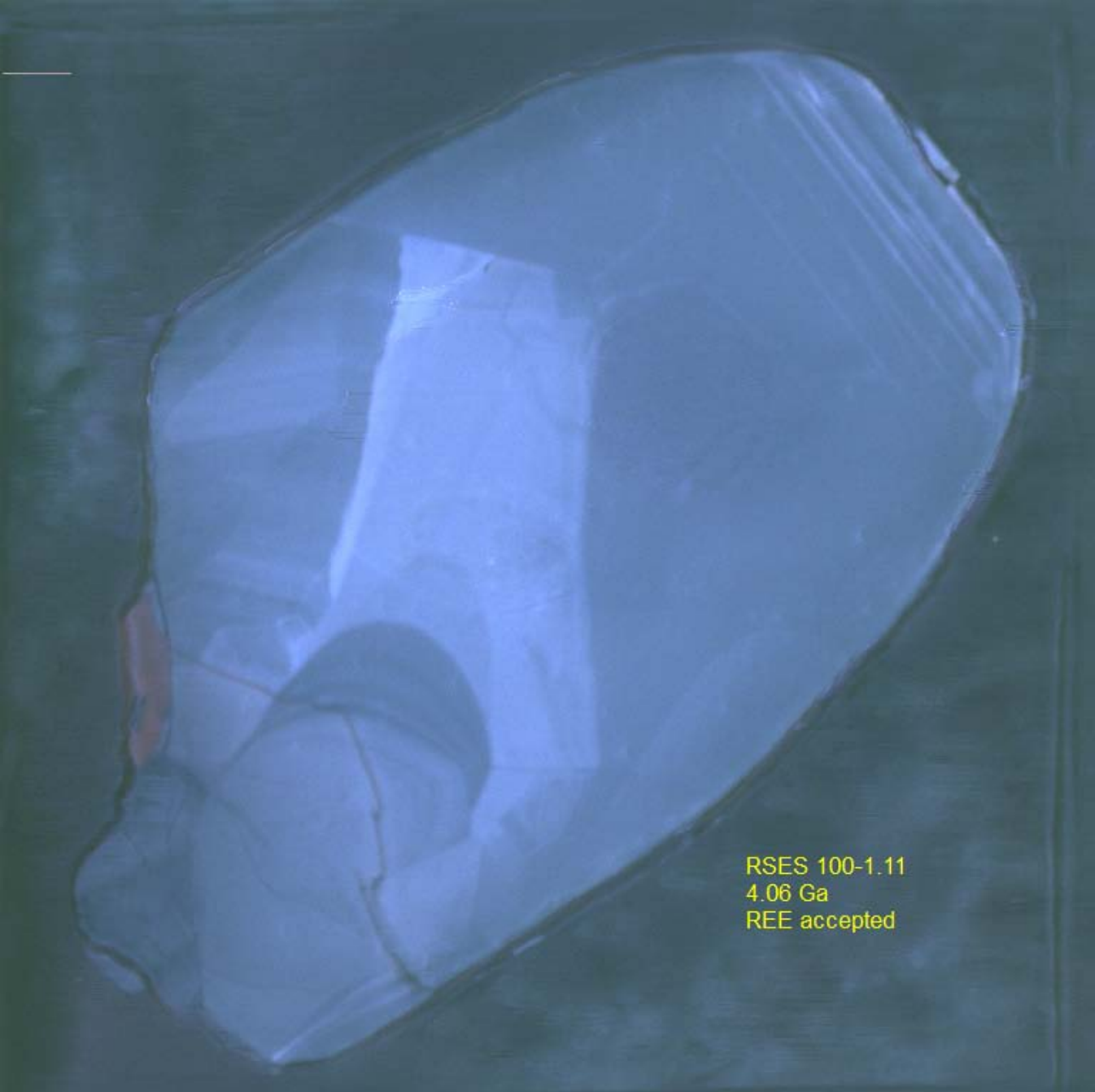
RSES 100-1.11
4.06 Ga
REE accepted

| SEM HV: 20.0 kV | WD: 17.32 mm | | VEGA3 TESCAN |
| View field: 232 µm | Det: Color CL | 50 µm | UCLA - EPSS |

RSES 100-1.12
3.95 Ga
REE accepted

SEM HV: 20.0 kV | WD: 17.25 mm | | VEGA3 TESCAN
View field: 280 µm | Det: Color CL | 50 µm | UCLA - EPSS

RSES 100-1.18
4.07 Ga
REE accepted
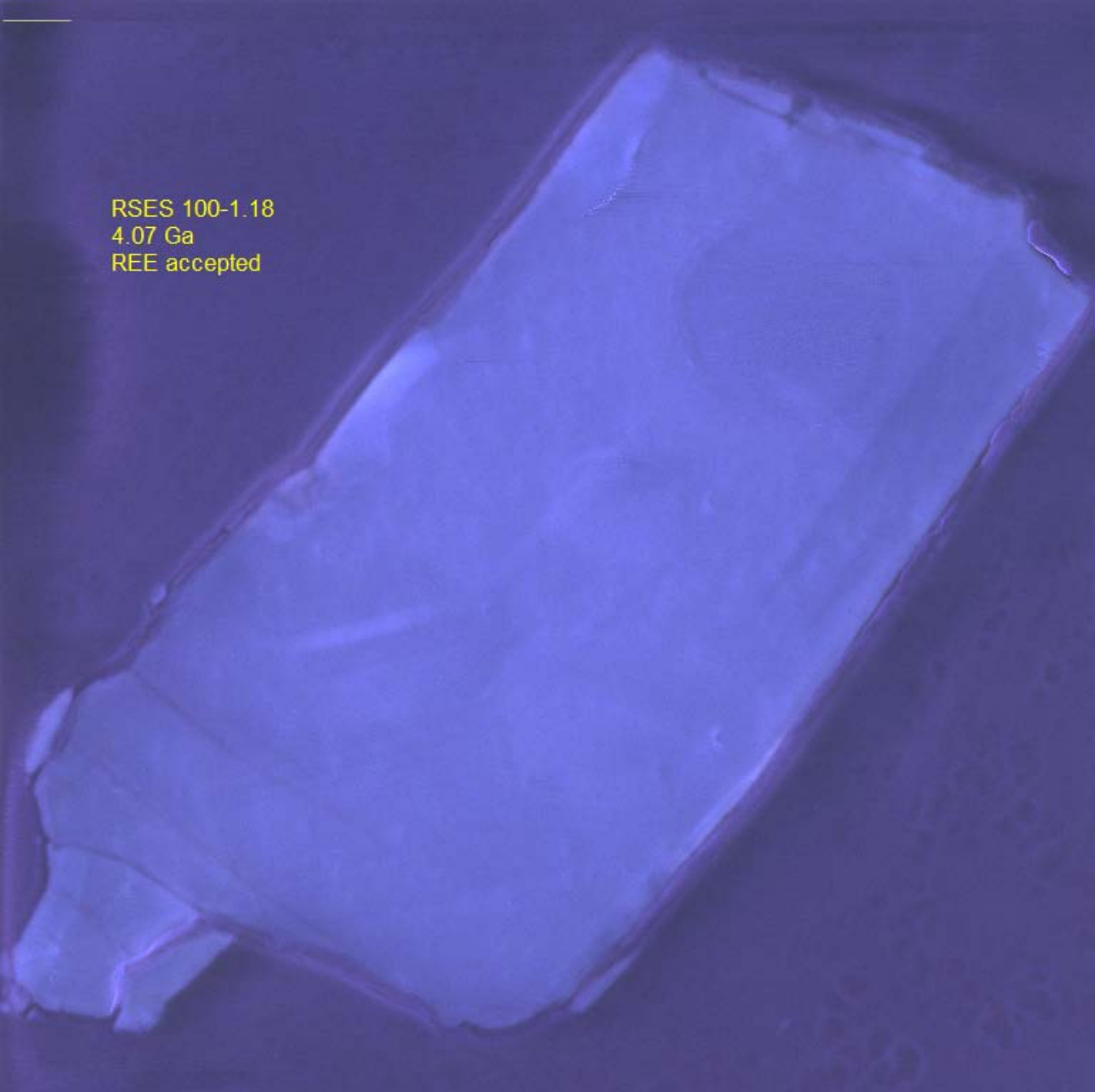
SEM HV: 20.0 kV | WD: 17.23 mm | | VEGA3 TESCAN
View field: 200 µm | Det: Color CL | 50 µm | UCLA - EPSS

RSES 100-15.2
4.09 Ga
REE accepted

SEM HV: 20.0 kV | WD: 17.30 mm | | VEGA3 TESCAN
View field: 183 µm | Det: Color CL | 50 µm | UCLA - EPSS

RSES 100-16.2
4.11 Ga
REE accepted
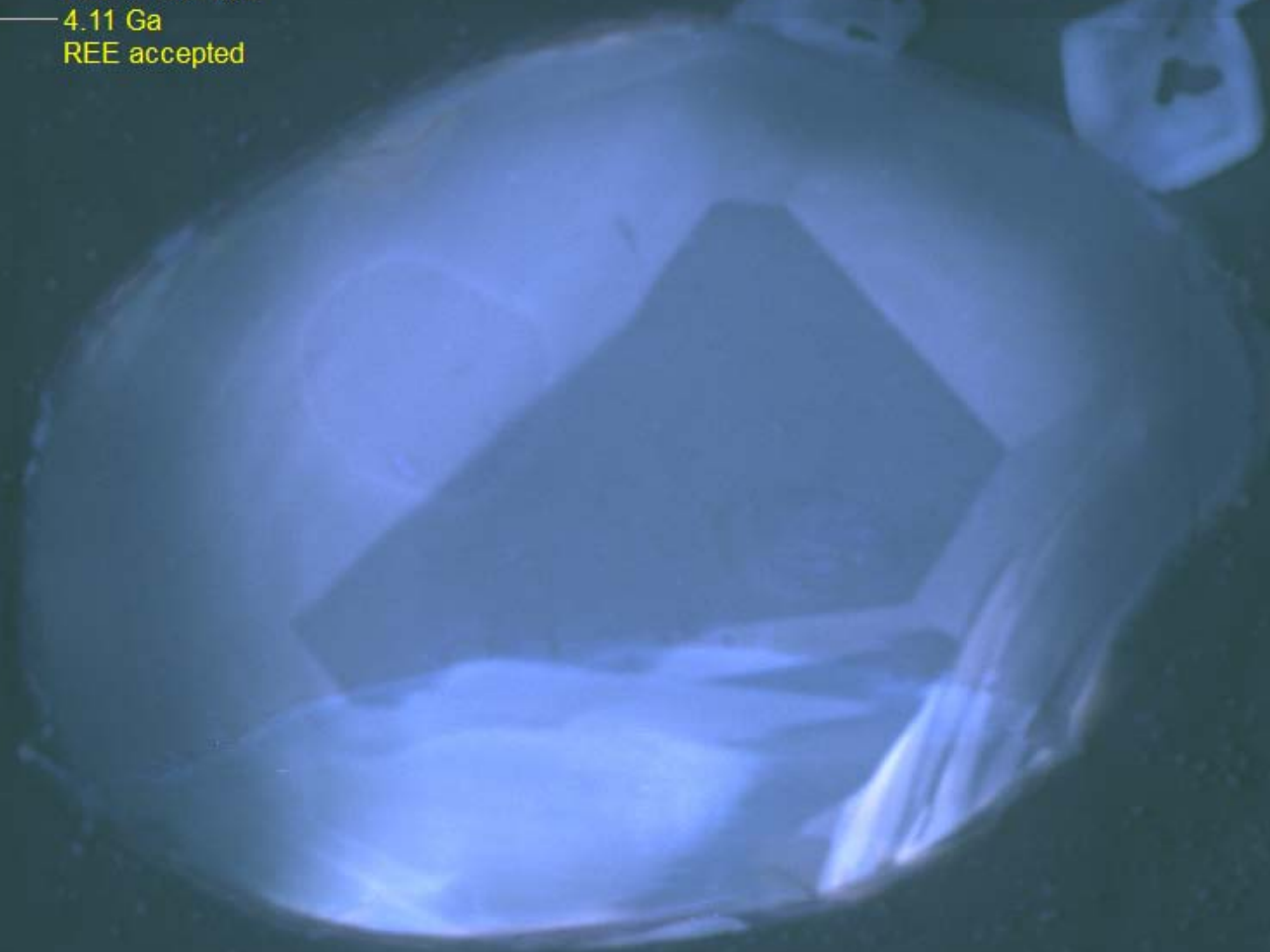
SEM HV: 20.0 kV | WD: 17.15 mm | | VEGA3 TESCAN
View field: 218 µm | Det: Color CL | 50 µm | UCLA - EPSS
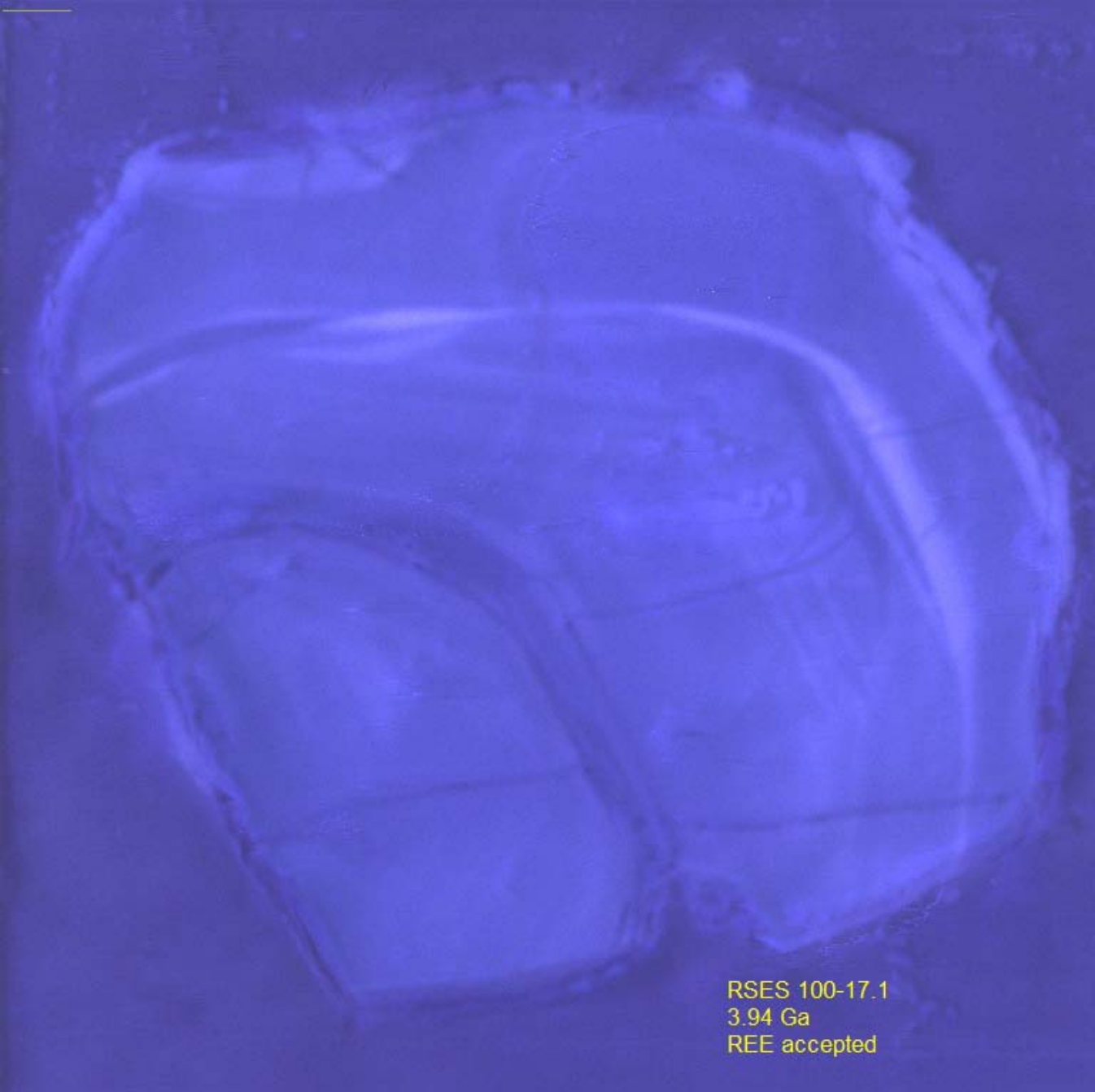
RSES 100-17.1
3.94 Ga
REE accepted

| SEM HV: 20.0 kV | WD: 17.31 mm | | VEGA3 TESCAN |
| View field: 148 µm | Det: Color CL | 20 µm | UCLA - EPSS |
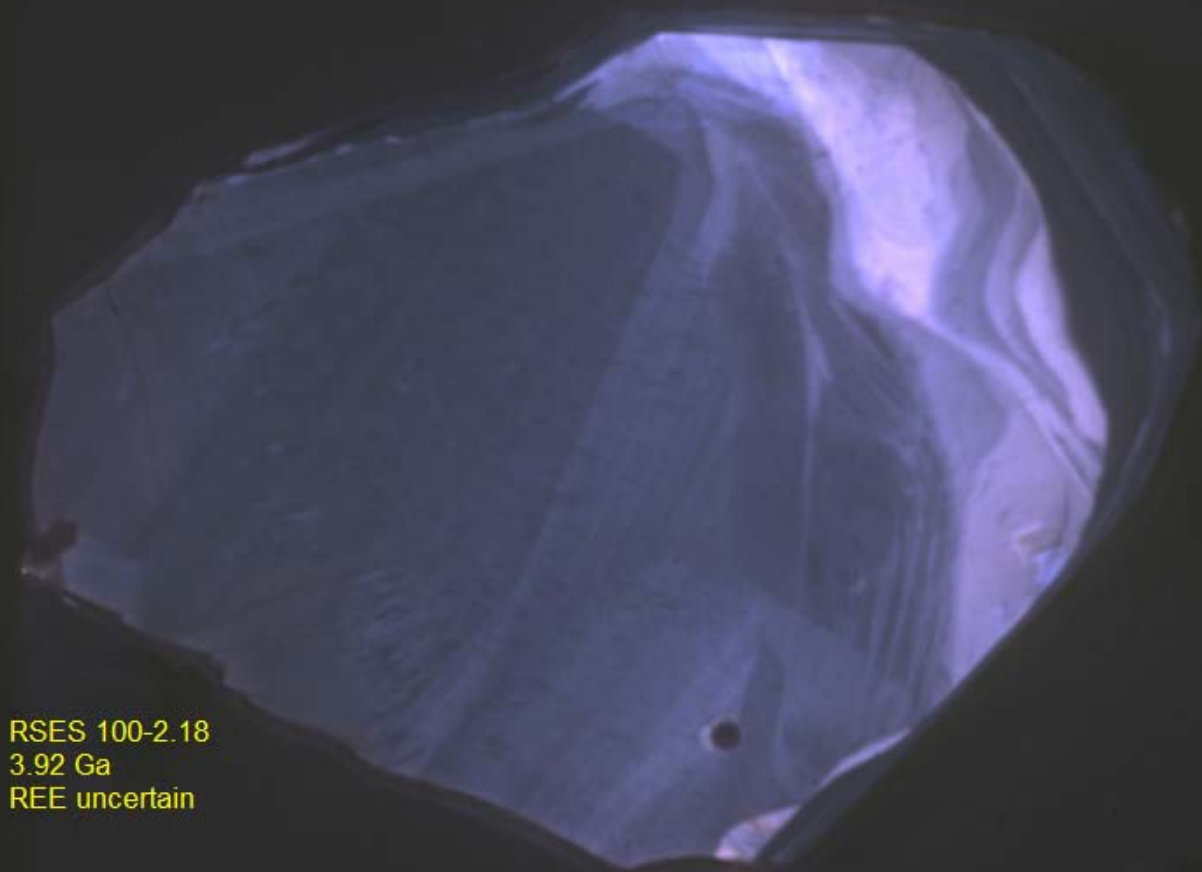
RSES 100-2.18
3.92 Ga
REE uncertain

SEM HV: 20.0 kV          WD: 17.41 mm                          VEGA3 TESCAN

View field: 309 µm      Det: Color CL          50 µm            UCLA - EPSS
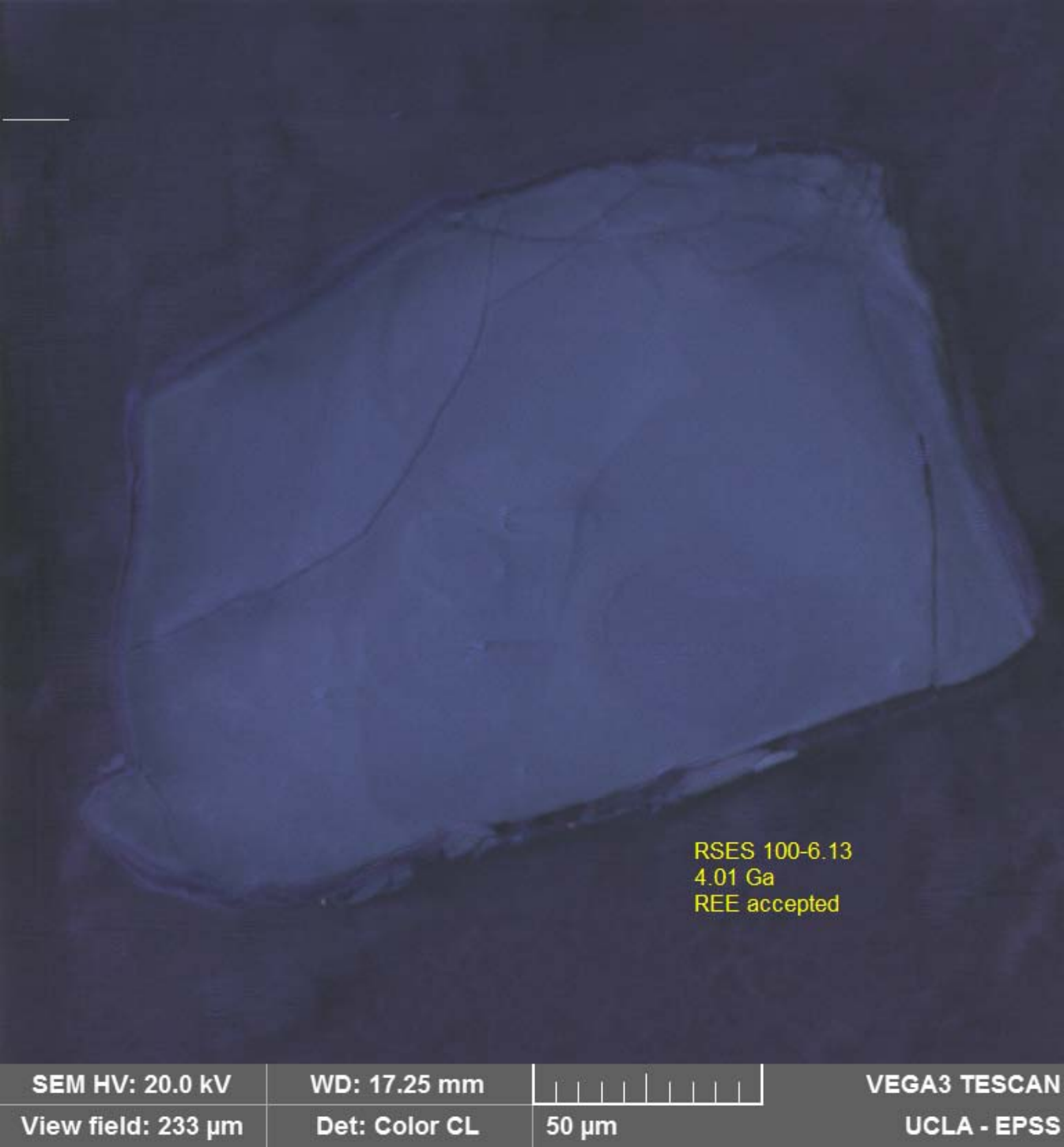
RSES 100-6.13
4.01 Ga
REE accepted

| SEM HV: 20.0 kV | WD: 17.25 mm | | VEGA3 TESCAN |
| View field: 233 µm | Det: Color CL | 50 µm | UCLA - EPSS |
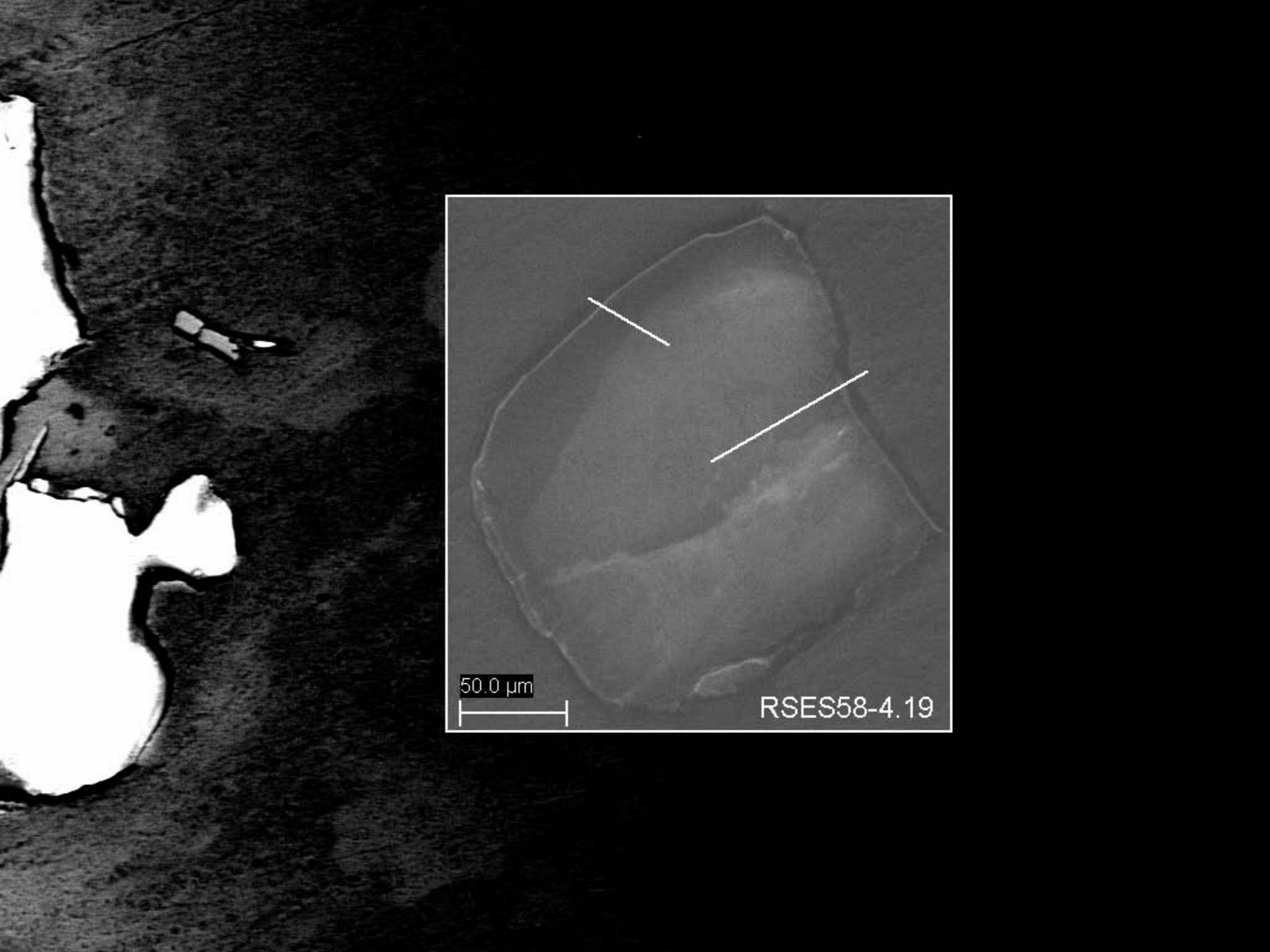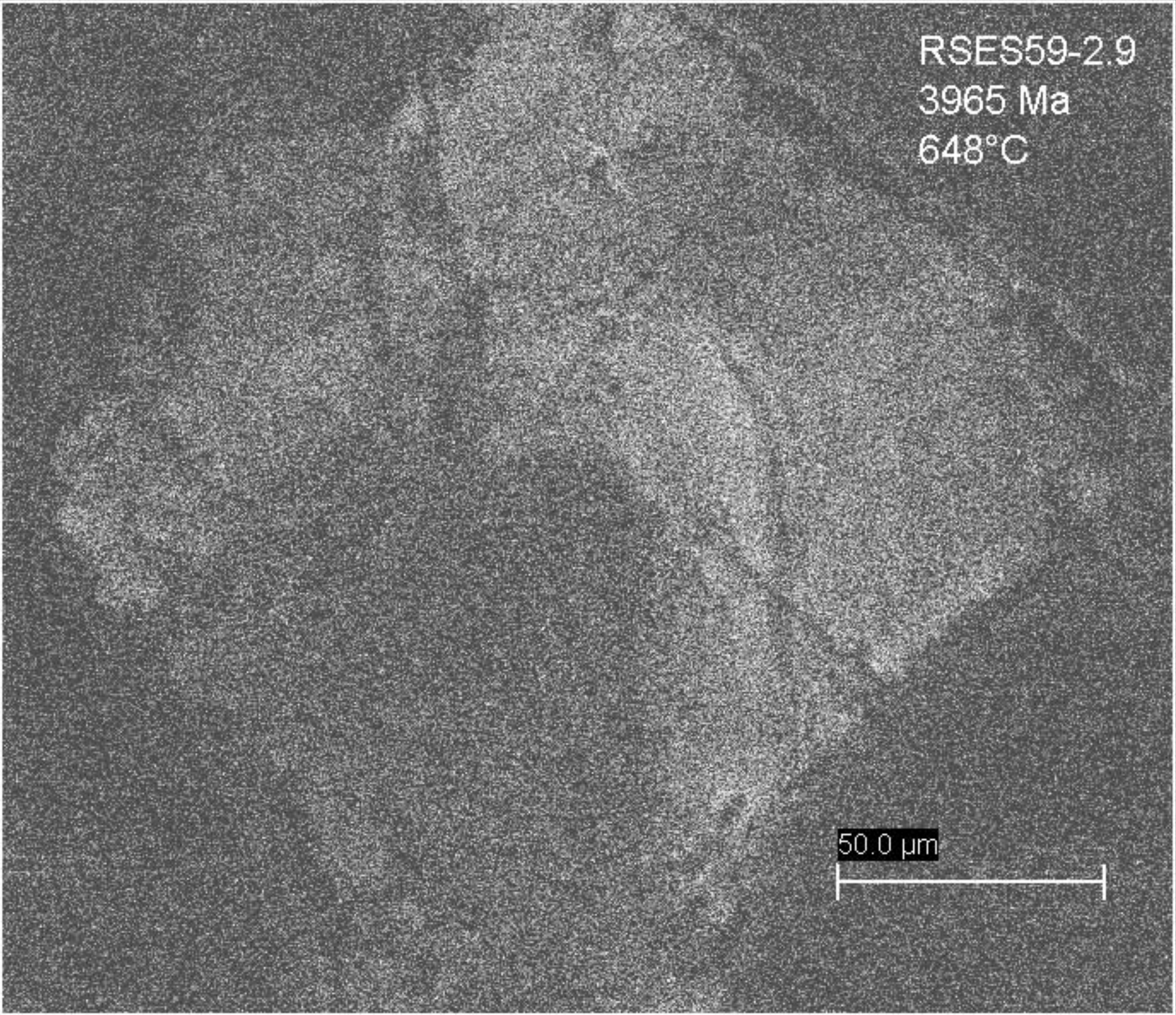
50.0 μm

RSES58-4.19

RSES59-2.9
3965 Ma
648°C

50.0 µm

RSES60-16.1

50.0 µm

spot

spot

RSES60-7.19

50.0 µm

spot

spot